

# TARGET TRANSFORMATION CONSTRAINED SPARSE UNMIXING (TTCSU) ALGORITHM FOR RETRIEVING HYDROUS MINERALS ON MARS: APPLICATION TO SOUTHWEST MELAS CHASMA

Honglei Lin<sup>1,2</sup>, Xia Zhang<sup>1,\*</sup>, Xing Wu<sup>1,2</sup>, J. D. Tarnas<sup>3</sup>, J. F. Mustard<sup>3</sup>

<sup>1</sup> Institute of Remote Sensing and Digital Earth, CAS, Beijing, 100101 - (linhl, zhangxia, wuxing) @radi.ac.cn

<sup>2</sup> University of Chinese Academy of Sciences, Beijing 100049, China

<sup>3</sup> Dept. of Earth, Environmental, and Planetary Sciences, Brown University, RI, 02912, USA.

## Commission VI, ICWG III/II

**KEY WORDS:** Prior information, Sparse unmixing, Hydrous minerals, Mars, CRISM

### ABSTRACT:

Quantitative analysis of hydrated minerals from hyperspectral remote sensing data is fundamental for understanding Martian geologic process. Because of the difficulties for selecting endmembers from hyperspectral images, a sparse unmixing algorithm has been proposed to be applied to CRISM data on Mars. However, it's challenge when the endmember library increases dramatically. Here, we proposed a new methodology termed Target Transformation Constrained Sparse Unmixing (TTCSU) to accurately detect hydrous minerals on Mars. A new version of target transformation technique proposed in our recent work was used to obtain the potential detections from CRISM data. Sparse unmixing constrained with these detections as prior information was applied to CRISM single-scattering albedo images, which were calculated using a Hapke radiative transfer model. This methodology increases success rate of the automatic endmember selection of sparse unmixing and could get more accurate abundances. CRISM images with well analyzed in Southwest Melas Chasma was used to validate our methodology in this study. The sulfates jarosite was detected from Southwest Melas Chasma, the distribution is consistent with previous work and the abundance is comparable. More validations will be done in our future work.

## 1. INTRODUCTION

The hydrous minerals on Mars preserve a record of potential past aqueous activity. Information regarding mineralogical composition would enable a better understanding of their formation environment, and provide unique insights into the geological evolution of Mars (Lin and Zhang 2017). Hyperspectral remotely sensed images generally have several hundreds of contiguous electromagnetic wavelengths, and they enable us to assess a dense spectrum in each pixel, making possible the identification and quantitative analysis of various minerals (Nakhostin et al. 2016). At present, there are vast amount of hyperspectral remote sensing data on Mars, including Thermal Emission Spectrometer (TES) (Christensen et al. 2001), Observatoire pour la Minéralogie, l'Eau, les Glaces, et l'Activité (OMEGA) (Bibring et al. 2005) and Compact Reconnaissance Imaging Spectrometer for Mars (CRISM) (Murchie et al. 2007). CRISM has the highest spatial and spectral resolution among these data, which greatly enhanced our knowledge about Martian mineralogy. Though the mineral identifications from hyperspectral remote sensing data can indicate the different aqueous environments on Mars, quantitative analysis can better constrain the formation of these minerals (Poulet et al. 2014, Edwards and Ehlmann 2016).

There are several efforts have been made to get quantitative mineral abundances using spectroscopy on Mars. Bandfield et al. (2002) used TES thermal infrared data to obtain the hematite,

pyroxene, silicate and sulfate on Martian surface. However, the spatial resolution of TES data is too low to locate the hydrous mineral accurately. In the Visible-Near infrared (VNIR) wavelength, the observed signal of reflected light from a particulate surface is a non-linear combination of the spectral properties of the minerals (Mustard and Pieters 1989). The widely used non-linear mixing models in planetary spectra study are Hapke radiative transfer model (Hapke 1981) and the geometric optics model of Shkuratov (Shkuratov et al. 1999). Both the Hapke and Shkuratov models have been used to retrieve mineral abundances from the VNIR spectra of Mars (Poulet et al. 2008, Poulet et al. 2014, Edwards and Ehlmann 2016). However, the identification of the endmember signatures in the original data set is always challenging. The commonly used endmember identification method is spectral parameters (Viviano-Beck et al. 2014) and visual inspection, which is subjective and time consuming. Sparse unmixing method proposed by Iordache et al. (2011) can select the optimal combination of spectra from a large endmember library to best model the image spectra in an unsupervised fashion, avoiding the endmember determination in advance. Sparse unmixing method has been applied to hydrous mineral abundance retrieval on Mars (Lin and Zhang 2017). However, the accuracy of abundance retrieval will be decreased as the increasing of endmember library. So, endmember library for sparse unmixing method should be constrained. A Dynamic Aperture Target Transformation (DATT) method proposed in our recent work based on Factor Analysis and Target Transformation (FATT) method (Liu et al. 2016) can identify specific minerals from

\* Corresponding author

Martian VNIR hyperspectral data. The DATT results can provide a priori spectral information within the CRISM scenes to enhance the performance of sparse unmixing method.

In this work, a new method named 'Target Transformation Constrained Sparse Unmixing (TTCSU)' was proposed to accurately retrieve the abundance distributions of hydrous minerals from CRISM data. First, an endmember library is carefully constructed. Then DATT method is used to get the priori information for sparse unmixing. At last, sparse unmixing constrained with DATT detections as *a priori* information was applied to CRISM single-scattering albedo images, which are calculated using a Hapke radiative transfer model.

## 2. STUDY AREA AND DATA SETS

### 2.1 Study Area

Melas Chasma is the widest segment of the Valles Marineris on Mars and is located in the center of this canyon system (Figure 1). It contains extensive and highly organized Hesperian-aged valley networks and alluvial fans. Our study site is located in southwest Melas Chasma, where close to an enclosed perched basin. A sequence of interbedded poly- and mono-hydrated sulfate and jarosite deposits were identified by Liu et al (Liu and Catalano 2016). Specifically, these hydrated sulfate deposits are interbedded and have been highly deformed. The interbedded layers are exposed at the bottom of the stratigraphic column, unconformably overlain by a thick monohydrated sulfate unit.

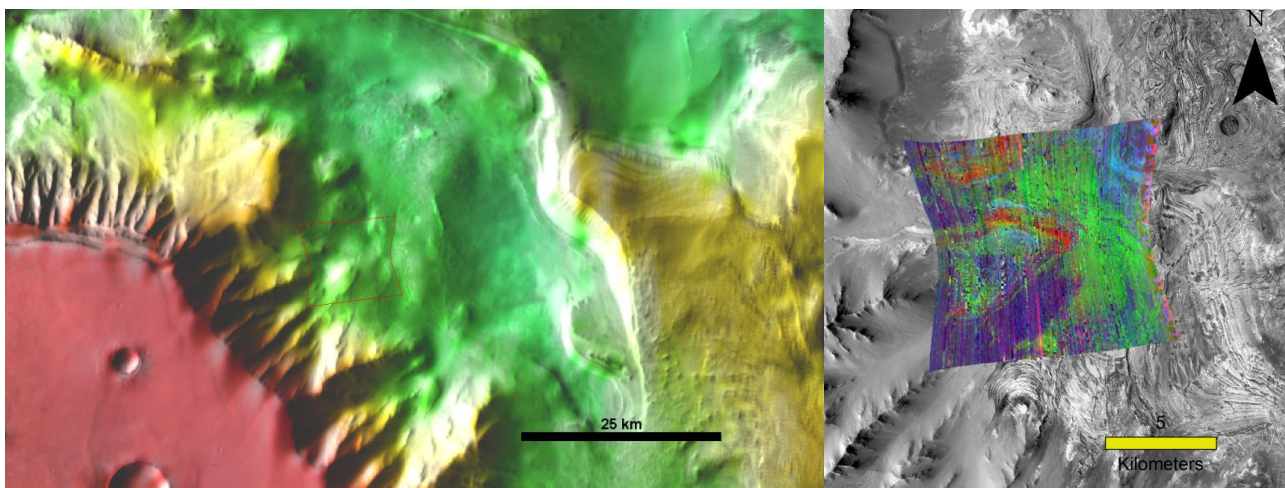


Figure. 1. Southwest Melas Chasma. (a) Regional context. The hill shaded map is produced from THEMIS day IR with MOLA color, the red outline is footprint of CRISM FRT00013F5B. (b) FRT00013F5B spectral parameters map overlain on CTX (R:BD2265, G: SINDEXT, B: BD2100). North is up in both images.

### 2.2 Data Sets

**2.2.1 CRISM data:** CRISM is a VNIR imaging spectrometer onboard the Mars Reconnaissance Orbiter (MRO). It covers the wavelength range of 0.36~3.94 $\mu\text{m}$ . In this paper, the CRISM targeted mode observation with full spatial resolution of 18 m/pixel, and a spectral sampling of 6.5 nm (Murchie et al. 2007) were used.

The CRISM image used in this study is FRT00013F5B. The pre-processing including photometrical and atmospheric correction was finished with the help of CRISM Analysis Toolkit (CAT). The image was photometrically corrected by dividing each spectrum by the cosine of the incidence angle. Then it was atmospherically corrected using the "Volcano Scan" method (Murchie et al. 2007). Although Volcano Scan technique does not remove aerosol contributions to spectra completely, it corrects the main atmospheric absorption caused by  $\text{CO}_2$ . The wavelength between 1~2.6 $\mu\text{m}$  were used in this study, because the primary spectral feature of hydrous minerals is within this range.

**2.2.2 CRISM Spectral Library:** The CRISM spectral library is a collection of laboratory spectra of Mars-analog materials supplied by the CRISM Team. The library was used to build endmember library for spectral unmixing. It contains 2463 spectral analyses of 1228 specimens, and all spectra were measured under desiccating conditions to remove atmospheric  $\text{H}_2\text{O}$  contamination, providing a better proxy to current desiccated Martian conditions. The naturally occurring minerals with valid spectra were selected. Finally, 139 samples were chosen to construct the endmember library. All spectra were resampled at the wavelength of the CRISM using linear interpolation. All the sulfates spectra in the endmember library were used to build a target library for DATT detection.

## 3. METHOD

Target Transformation Constrained Sparse Unmixing (TTCSU) was proposed in this study to get more reliable mineral abundance from VNIR hyperspectral remote sensing data. The flowchart of TTCSU is shown in Figure. 2. First, an endmember library is carefully constructed based on CRISM spectral library. Then DATT method is used to detect the possible presence of the specific minerals. DATT detections will be the priori information for sparse unmixing. At last, sparse unmixing constrained with DATT detections as a priori information was applied to CRISM single-scattering albedo images, which are calculated using a Hapke radiative transfer model.

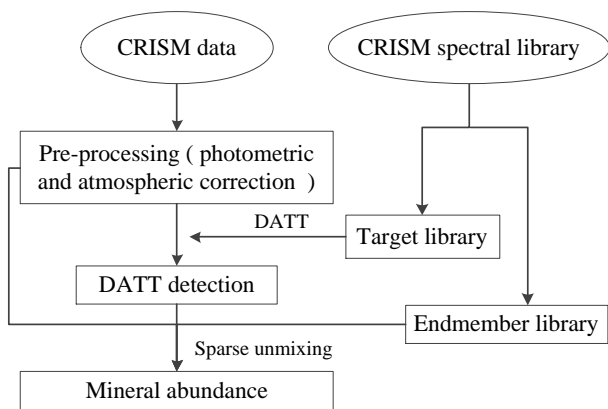


Figure. 2. The flowchart of TTCSU method.

### 3.1 Dynamic Aperture Target Transformation

Dynamic Aperture Target Transformation (DATT) is inspired by Factor Analysis and Target Transformation (FATT), it alleviates several key limitations in FATT and has the potential to test for specific minerals on Mars. The DATT method includes three steps: 1) Using the Hyperspectral signal identification by minimum error (Hysime) algorithm to determine important eigenvectors objectively. 2) Normalizing library and modeled spectra to allow for RMSE comparison between minerals with different reflectance scales, allowing for robust assessment of fit quality. 3) Using a dynamic aperture to detect minerals from hyperspectral data on Mars. Rather than analyzing an entire CRISM scene for a specific mineral, we analyze specific sets of pixels within our moving and dynamically shaped aperture. The pixels in which detections from all the differently shaped apertures intersect are considered as true detections.

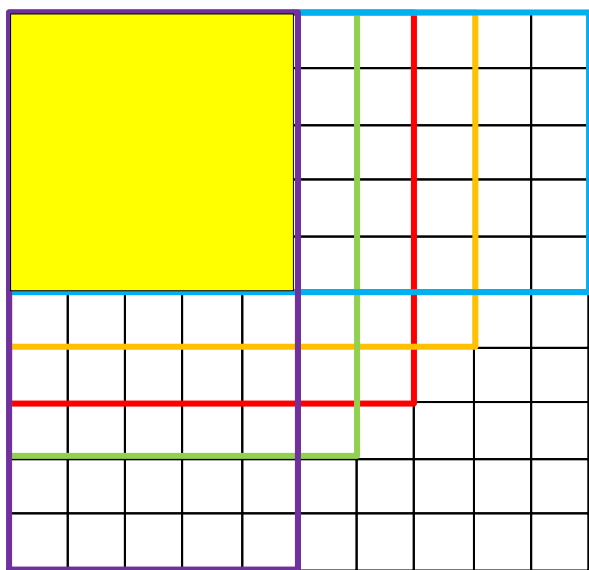


Figure. 3. The illustration of DATT. FATT is applied to all pixel subsets (blue, orange, red, green and purple) and if all the apertures return detections, the pixels in the yellow part are considered as true detections.

### 3.2 Single-Scattering Albedo Retrieval

Single-Scattering Albedo (SSA) is the ratio of scattered light to total extinct light. Hapke bidirectional reflectance distribution function relates the reflectance of a mixture to a linear combination of the SSA of its constituent endmembers. It

enables us to perform linear mixture analysis of the observed spectra (Goudge et al. 2015, Liu et al. 2016, Lin and Zhang 2017). The function is described as the following equation (Hapke 1981):

$$r(i, e, g) = \frac{\omega}{4} \frac{\mu_0}{(\mu_0 + \mu)} [(1 + B(g))P(g) + H(\mu_0)H(\mu) - 1] \quad (1)$$

$$H(\mu) = \frac{1 + 2\mu}{1 + 2\mu\sqrt{1 - \omega}} \quad (2)$$

where  $r(i, e, g)$  is the radiance factor, equivalent to CRISM I/F;  $i$ ,  $e$ , and  $g$  are incidence, emergence, and phase angles, respectively;  $\omega$  is the average single particle scattering albedo;  $B(g)$  is the backscattering function at the phase angle  $g$ ;  $P(g)$  is the surface phase function;  $H$  is the Chandrasekhar integral function associated with the observation geometry.

In this work, we assumed that  $P(g)=1$ , which implies that the surface scatters isotropically. The model is also on the assumption that there is no opposition effect. Because the opposition effect is strongest for phase angles  $<15^\circ$  (Mustard and Pieters 1989), and our data are at phase angles  $\geq 30^\circ$ . Thus,  $B(g)=0$ ; The effect of anisotropic scattering on abundance estimates for binary and ternary mixtures is about 5–10% when measured at phase angles of 15–120 (Mustard and Pieters 1989). Therefore, we can convert reflectance of CRISM images and spectral library to SSA with analytic solution of equation (1):

$$\sqrt{1 - \omega} = \frac{[(\mu_0 + \mu)^2 \Gamma_L^2 + (1 + 4\mu_0 \mu \Gamma_L)(1 - \Gamma_L)]^{1/2} - (\mu_0 + \mu) \Gamma_L}{1 + 4\mu_0 \mu \Gamma_L} \quad (3)$$

$$\Gamma_L = 4 \frac{\mu_0 + \mu}{\mu_0} \frac{1}{(1 + 2\mu_0)(1 + 2\mu)} r \quad (4)$$

The SSA of minerals can be added linearly:

$$\omega_{mix} = \sum_{i=1}^K F_i \omega_i \quad (5)$$

$F$  is the abundance of each component in the mixture.

### 3.3 Sparse Unmixing Using Spectral A Priori Information

Sparse unmixing (SU) is an active research area in hyperspectral unmixing in recent years (Iordache et al. 2011, Iordache et al. 2014), which aims to find the optimal subset of signatures in a spectral library that can best model hyperspectral data. A sparsity regularizer is commonly imposed to promote the number of selected signatures as small as possible. However, the high mutual coherence of spectral library limits the performance of SU. In practice, it assumes that some materials in the spectral library are known to exist in the scene. Tang et al. (2015) incorporated the spectral a priori information into SU, presented a new algorithm, which is termed sparse unmixing using spectral a priori information (SU<sub>n</sub>SPI), the problem can be written as equation:

$$\min_x \frac{1}{2} \|AX - Y\|_F^2 + \lambda_s \|X\|_1 + \lambda_p \|HX\|_{2,1} + \kappa_{R^+}(X) \quad (6)$$

where  $Y$  is the measured spectra of the pixels ( $L$  bands,  $K$  pixels),  $Y \in R^{L \times K}$ ;  $X$  is the abundance matrix corresponding to reflectance spectral library ( $L$  bands,  $m$  signatures),  $A \in R^{L \times m}$ ,

$X \in R^{m \times K}$ ;  $\lambda_s \geq 0$  and  $\lambda_p \geq 0$  are regularization parameters.  $H \in R^{m \times m}$  is a diagonal matrix related to the set of priori:

$$h_{ii} = \begin{cases} 0, & \text{if } i \in \text{Priori} \\ 1, & \text{otherwise} \end{cases} \quad (7)$$

$\|X\|_1 = \sum_{i=1}^K \|x_i\|_1$  denotes the  $\ell_1$  norm, this term enforces each column of  $X$  to be sparse;  $\|X\|_{2,1} = \sum_{k=1}^m \|x^k\|_2$  denotes the  $\ell_{2,1}$  norm, this term is proposed to enforce the row-sparsity;  $\kappa_{R^+}(X) = \sum_{j=1}^n \kappa_{R^+}(x_j)$ ,  $x_i$  represents the  $i$ -th column, this term is an indicator function ( $\kappa_{R^+}(x_i)$  is zero if  $x_i$  belongs to the nonnegative orthant, otherwise  $\kappa_{R^+}(x_i)$  is infinity). The optimization problem in (3) can be solved via alternating direction method of multipliers (ADMM).

Here, the sparse unmixing is performed pixel by pixel. The DATT detections of each pixel are the priori information for sparse unmixing.

## 4. RESULTS

### 4.1 TTCSU results

According to TTCSU results in FRT00013F5B, the major hydrous sulfates are jarosite, poly-hydrated sulfate and szomolnokite. As shown in Figure.4, the abundances of sulfates are related to CRISM parameter values, indicating our abundance results are linear correlated to the strength of absorption features. The abundance distribution of sulfates is consistent with topography. The fits between measured and TTCSU modeled spectra are very good, as shown in Figure.4g-i.

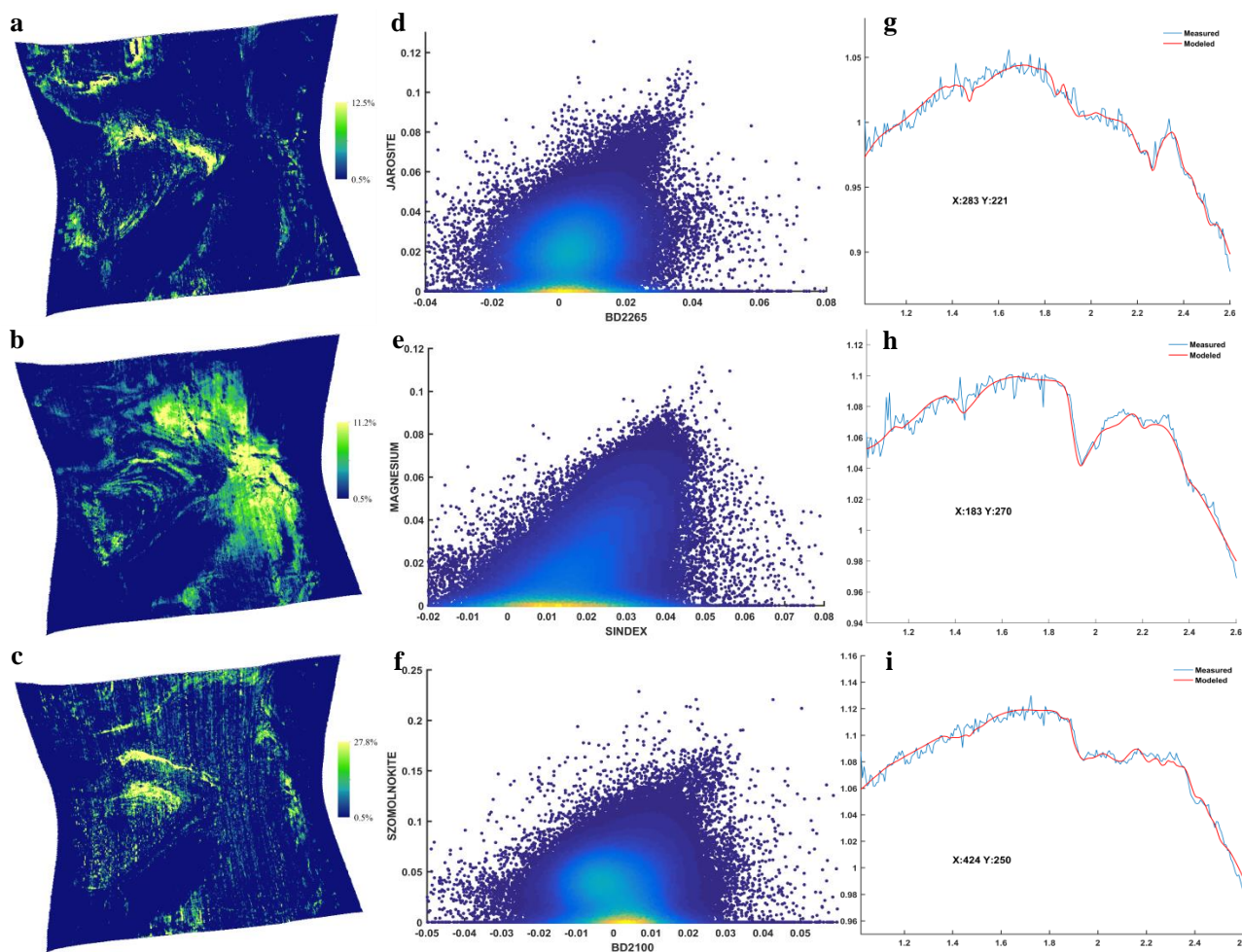


Figure. 4. The abundance map of hydrous sulfates in Southwest Melas Chasma. a) Jarosite abundance map. b) Poly-hydrated sulfate abundance. c) Szomolnokite abundance map. d) The correlation between jarosite abundance and BD2265. e) The correlation between poly-hydrated sulfate abundance and SINDEXT. f) The correlation between szomolnokite abundance and BD2100. g) TTCSU fit of pixels with high abundance jarosite. h) TTCSU fit of pixels with high abundance poly-hydrated sulfate. i) TTCSU fit of pixels with high abundance szomolnokite.

### 4.2 Validation of results

The spectra of jarosite, poly-hydrated sulfate and szomolnokite with highest abundance were extracted using ratio technique, as shown in Figure. 5. The comparison with library spectra shows

that the ratio spectra in the high abundance region have the main spectral feature of the corresponding sulfate. The exact mineral spectra directly extracted from CRISM image based on our abundance results verified the validation of TTCSU method.

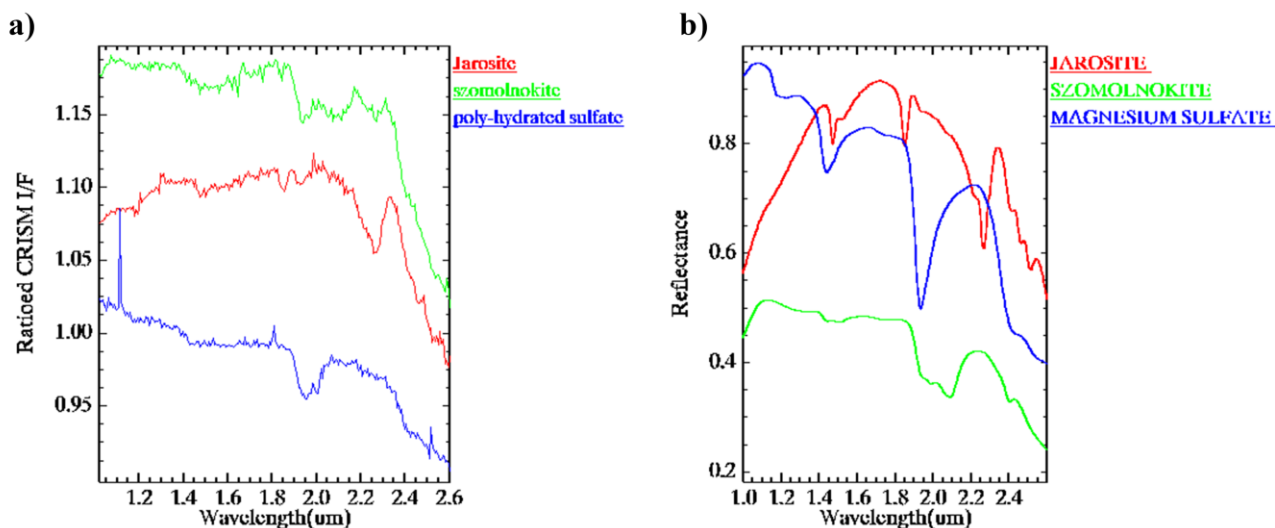


Figure. 5. a) The ratio spectra of jarosite, poly-hydrated sulfate and szomolnokite. b) The library spectra.

Using Hapke model and least square method, Liu, et al. (2016) got the jarosite abundance map (Figure. 6b) in FRT00003F5B, which is similar with our result (Figure. 4a), especially in the high abundance regions. The szomolnokite wasn't detected in their works because of the lack of endmembers in the

endmember library. However, according to the DATT fits, TTCSU fits and ratio spectra, the szomolnokite is a possible mineral in FRT00003F5B.

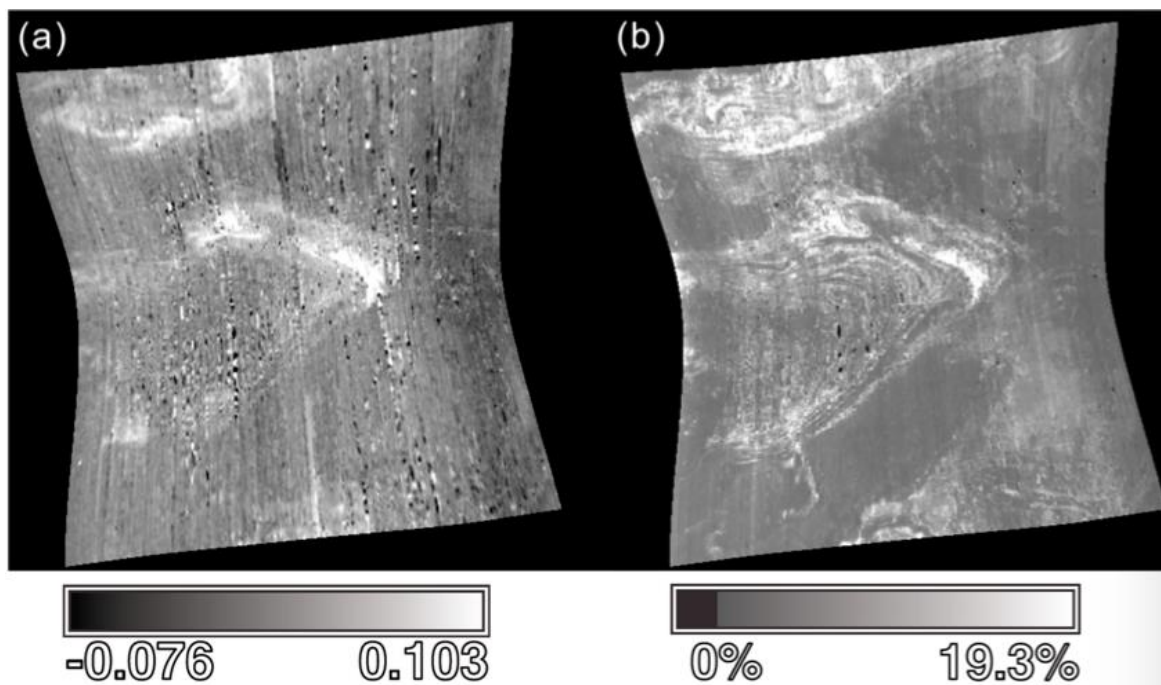


Figure. 6. The jarosite distribution in FRT00013F5B (Liu et al. 2016). a) CRISM parameter index map for Jarosite b) Modeled jarosite abundance.

### 5. CONCLUSIONS

Target transformation constrained sparse unmixing method for hydrous mineral retrieval was proposed in this paper. The preliminary application to CRISM image shows the good performance of TTCSU method. In Southwest Melas Chasma, jarosite, poly-hydrated sulfate and szomolnokite are detected, which are validated by extracting spectra from image and comparing with previous studies. More CRISM images should be used to verify TTCSU in the future work.

### ACKNOWLEDGEMENTS

The authors are very grateful for the financial support provided by the National Natural Science Foundation of China (grant no.41671360).

### REFERENCES

Bandfield, J. L., 2002. Global mineral distributions on Mars. *Journal of Geophysical Research-Planets*, 107(E6).

- Bibring, J. P., Y. Langevin, A. Gendrin, B. Gondet, F. Poulet, M. Berthe, A. Soufflot, R. Arvidson, N. Mangold, J. Mustard, P. Drossart and O. Team, 2005. Mars surface diversity as revealed by the OMEGA/Mars Express observations. *Science*, 307(5715), pp. 1576-1581.
- Christensen, P. R., J. L. Bandfield, V. E. Hamilton, S. W. Ruff, H. H. Kieffer, T. N. Titus, M. C. Malin, R. V. Morris, M. D. Lane, R. L. Clark, B. M. Jakosky, M. T. Mellon, J. C. Pearl, B. J. Conrath, M. D. Smith, R. T. Clancy, R. O. Kuzmin, T. Roush, G. L. Mehall, N. Gorelick, K. Bender, K. Murray, S. Dason, E. Greene, S. Silverman and M. Greenfield, 2001. Mars Global Surveyor Thermal Emission Spectrometer experiment: Investigation description and surface science results. *Journal of Geophysical Research-Planets*, 106(E10), pp. 23823-23871.
- Edwards, C. S. and B. L. Ehlmann, 2016. Carbon sequestration on Mars. *Geology*, 44(6), pp. E389-E389.
- Goudge, T. A., J. F. Mustard, J. W. Head, M. R. Salvatore and S. M. Wiseman, 2015. Integrating CRISM and TES hyperspectral data to characterize a halloysite-bearing deposit in Kashira crater, Mars. *Icarus*, 250, pp. 165-187.
- Hapke, B., 1981. Bidirectional Reflectance Spectroscopy .1. Theory. *Journal of Geophysical Research*, 86(Nb4), pp. 3039-3054.
- Iordache, M. D., J. M. Bioucas-Dias and A. Plaza (2011). "Sparse Unmixing of Hyperspectral Data." *Ieee Transactions on Geoscience and Remote Sensing*, 49(6), pp. 2014-2039.
- Iordache, M. D., J. M. Bioucas-Dias, A. Plaza and B. Somers, 2014. MUSIC-CSR: Hyperspectral Unmixing via Multiple Signal Classification and Collaborative Sparse Regression. *Ieee Transactions on Geoscience and Remote Sensing*, 52(7), pp. 4364-4382.
- Lin, H. and X. Zhang, 2017. Retrieving the hydrous minerals on Mars by sparse unmixing and the Hapke model using MRO/CRISM data. *Icarus*, 288, pp. 160-171.
- Liu, Y. and J. G. Catalano, 2016. Implications for the aqueous history of southwest Melas Chasma, Mars as revealed by interbedded hydrated sulfate and Fe/Mg-smectite deposits. *Icarus*, 271, pp. 283-291.
- Liu, Y., T. D. Glotch, N. A. Scudder, M. L. Kraner, T. Condu, R. E. Arvidson, E. A. Guinness, M. J. Wolff and M. D. Smith, 2016. End-member identification and spectral mixture analysis of CRISM hyperspectral data: A case study on southwest Melas Chasma, Mars. *Journal of Geophysical Research-Planets*, 121(10), pp. 2004-2036.
- Murchie, S., R. Arvidson, P. Bedini, K. Beisser, J. P. Bibring, J. Bishop, J. Boldt, P. Cavender, T. Choo and R. T. Clancy, 2007. Compact Reconnaissance Imaging Spectrometer for Mars (CRISM) on Mars Reconnaissance Orbiter (MRO). *Journal of Geophysical Research Atmospheres*, 112(E5), pp. 431-433.
- Murchie, S., R. Arvidson, P. Bedini, K. Beisser, J. P. Bibring, J. Bishop, J. Boldt, P. Cavender, T. Choo, R. T. Clancy, E. H. Darlington, D. D. Marais, R. Espiritu, D. Fort, R. Green, E. Guinness, J. Hayes, C. Hash, K. Heffernan, J. Hemmler, G. Heyler, D. Humm, J. Hutcheson, N. Izenberg, R. Lee, J. Lees, D. Lohr, E. Malaret, T. Martin, J. A. McGovern, P. McGuire, R. Morris, J. Mustard, S. Pelkey, E. Rhodes, M. Robinson, T. Roush, E. Schaefer, G. Seagrave, F. Seelos, P. Silverglate, S. Slavney, M. Smith, W. J. Shyong, K. Strohhahn, H. Taylor, P. Thompson, B. Tossman, M. Wirzburger and M. Wolff, 2007. Compact reconnaissance Imaging Spectrometer for Mars (CRISM) on Mars Reconnaissance Orbiter (MRO). *Journal of Geophysical Research-Planets*, 112(E5).
- Mustard, J. F. and C. M. Pieters, 1989. Photometric Phase Functions of Common Geologic Minerals and Applications to Quantitative-Analysis of Mineral Mixture Reflectance Spectra. *Journal of Geophysical Research-Solid Earth and Planets*, 94(B10), pp. 13619-13634.
- Nakhostin, S., H. Clenet, T. Corpetti and N. Courty, 2016. Joint Anomaly Detection and Spectral Unmixing for Planetary Hyperspectral Images. *IEEE Transactions on Geoscience & Remote Sensing*, 54(12), pp. 6879-6894.
- Poulet, F., J. Carter, J. L. Bishop, D. Loizeau and S. M. Murchie, 2014. Mineral abundances at the final four curiosity study sites and implications for their formation. *Icarus*, 231, pp. 65-76.
- Poulet, F., N. Mangold, D. Loizeau, J. P. Bibring, Y. Langevin, J. Michalski and B. Gondet, 2008. Abundance of minerals in the phyllosilicate-rich units on Mars. *Astronomy & Astrophysics*, 487(2), pp. L41-U193.
- Shkuratov, Y., L. Starukhina, H. Hoffmann and G. Arnold, 1999. A model of spectral albedo of particulate surfaces: Implications for optical properties of the moon. *Icarus*, 137(2), pp. 235-246.
- Viviano-Beck, C. E., F. P. Seelos, S. L. Murchie, E. G. Kahn, K. D. Seelos, H. W. Taylor, K. Taylor, B. L. Ehlmann, S. M. Wisemann, J. F. Mustard and M. F. Morgan, 2014. Revised CRISM spectral parameters and summary products based on the currently detected mineral diversity on Mars. *Journal of Geophysical Research-Planets*, 119(6), pp. 1403-1431.